Atmospheric Environment 42 (2008) 6884–6896

Contents lists available at ScienceDirect

Atmospheric Environment

journal homepage: www.elsevier.com/locate/atmosenv

Study on an intense dust storm over Greece

D.G. Kaskaoutis [a], H.D. Kambezidis [a,*], P.T. Nastos [b], P.G. Kosmopoulos [b]

[a] Atmospheric Research Team, Institute for Environmental Research and Sustainable Development, National Observatory of Athens, Lofos Nymphon, P.O. Box 20048, GR-11810 Athens, Greece

[b] University of Athens, Department of Geology and Geoenvironment, University campus, GR-15784 Athens, Greece

ARTICLE INFO

Article history:
Received 7 February 2008
Received in revised form 2 May 2008
Accepted 7 May 2008

Keywords:
Saharan dust event
MODIS
Sunphotometer
PM_{10}
Eastern Mediterranean
Greece

ABSTRACT

Springtime constitutes the most favorable period for Sahara dust outbreaks and transport over Eastern Mediterranean. This study investigates the aerosol properties during April 2005 using remote-sensing and ground-based measurements. Three dust events with high aerosol optical depth (AOD) values have been observed during the measuring period, with duration of two days, i.e. 11–12, 16–17 and 25–26 April 2005. In this paper we mainly focus on the intense dust event of 16–17 April 2005, when a thick dust layer transported from Libya affected the whole Greek territory. Very high AOD values obtained from Aqua-MODIS sensor were observed over Greece (mean 2.42 ± 1.25) on 17 April, while the respective mean April value was 0.31 ± 0.09. The AOD at 550 nm (AOD_{550}) values over Crete were even larger, reaching ~4.0. As a consequence, the PM_{10} concentrations over Athens dramatically increased reaching up to 200 $\mu g\,m^{-3}$. On the other hand, the fine-mode fraction values obtained from Terra-MODIS showed a substantial decrease in the whole Greek area on 17 April with values below 0.2 in the Southern regions. The intense dust layer showed a complex behavior concerning its spatial and temporal evolution and allowed us to study the changes in the optical properties of the desert dust particles along their transport routes due to the mixing processes with other aerosol types. The results from different measurements (ground-based and remote-sensing) did not contradict each other and, therefore, are adequate for monitoring of dust load over the Eastern Mediterranean.

1. Introduction

According to the Earth Observatory (website http://earthobservatory.nasa.gov/intense) dust outbreaks are considered natural hazards, which affect the global and regional radiative balance (Satheesh and Krishna Moorthy, 2005 and references therein), cloud microphysical properties (Levin and Ganor, 1996), atmospheric heating and stability (Alpert et al., 2004), tropical cyclone activity (Dunion and Velden, 2004), ecosystems, marine environments and phytoplankton (Donaghay et al., 1991), photolysis rates and ozone chemistry (Zerefos et al., 2002), and human health (Rodriguez et al., 2001). Desert aerosols are probably the most abundant and massive type of aerosol particles that are present in the atmosphere worldwide. Therefore, dust, which is a common aerosol type over deserts (Ogunjobi et al., 2008), is considered to be one of the major sources of tropospheric aerosol loading, and constitutes an important key parameter in climate aerosol forcing studies (Kaufman et al., 2002). Mineral and desert dust play important roles in the radiative forcing, with an estimated Top of Atmosphere (TOA) radiative forcing in the range –0.6 to 0.4 $W\,m^{-2}$ (IPCC, 2007). However, the radiative forcing caused by dust particles is very uncertain in both magnitude and sign, mainly triggered by the chemical composition of mineral particles (Claquin et al., 1998), the wavelength dependence of their optical properties (like single-scattering albedo or SSA in brevity, asymmetry factor) as

* Corresponding author. Tel.: +30 210 3490119; fax: +30 210 3490113.
E-mail address: harry@meteo.noa.gr (H.D. Kambezidis).

1352-2310/$ – see front matter © 2008 Elsevier Ltd. All rights reserved.
doi:10.1016/j.atmosenv.2008.05.017

well as by the albedo of the underlying surface and also the relative height between the dust layer and the clouds (Kinne and Pueschel, 2001). Desert dust can be transported over long distances from the source regions (Prospero et al., 2002), with the larger particles to be deposited near the source, while the smaller ones to be suspended in the air for a few days or weeks, thus traveling over large distances.

The Sahara desert is the most important dust source in the world. Exports of dust plumes to the North Atlantic and Mediterranean Sea occur throughout the year (Moulin et al., 1998). While most (about 60%) of the Saharan dust is transported westward, a significant amount reaches Europe. On a regular annual basis, about 80–120 Tg of dust are transported to the Mediterranean (d' Almeida, 1986). The residence time of dust particles depends on the meteorological conditions, wind speed and precipitation that favor the dry and wet deposition, respectively. The occurrence of Sahara dust (SD) events above Mediterranean has a marked seasonal cycle, mainly driven by the intense cyclones called Sharav, south of the Atlas Mountains (Morocco). These cyclones are generated by the thermal contrast between cold Atlantic air and warm continental air that both cross North Africa during spring and summer (Moulin et al., 1998; Rodriguez et al., 2001). In spring the Sharav cyclones carry desert dust towards Eastern Mediterranean, while in summer the most intense activity occurs in the central part; by the end of the summer a low-pressure system over the Balearic Islands drives the dust plumes towards the Western Mediterranean (Meloni et al., 2007).

Therefore, there is a growing interest in examining the spatio-temporal aerosol dust distribution over Eastern Mediterranean and coastal Greece due to their proximity to the North African arid regions. The dust climatology over Mediterranean is mainly investigated via satellite sensors (Moulin et al., 1998; Israelevich et al., 2002; Antoine and Nobileau, 2006) due to their large spatial coverage. Moreover, extensive analysis about dust optical properties has been conducted over coastal Greece via sunphotometers (Fotiadi et al., 2006), lidar (Balis et al., 2004; Papayannis et al., 2005), and particle samplers (Gerasopoulos et al., 2006). The dust events over Greece occur either in an upper atmospheric level or in the whole atmospheric column, with the latter to be more intense, directly influencing the PM concentrations at the surface (Kalivitis et al., 2007).

The transport of SD to the Mediterranean and coastal Europe has been investigated, either as a climatological analysis or as "case studies" employing ground-based instrumentation, sunphotometers, particle samplers, lidar and satellite observations. In this paper, a combination of column-integrated aerosol optical and physical properties obtained from Terra- and Aqua-MODIS as well as by TOMS and OMI satellite sensors, and AERONET sunphotometer measurements were used to investigate the aerosol properties over Greece in April 2005, and more specifically, to study an intense dust event occurred on 16–17 April 2005. MODIS data were used over areas with different proximity to the North African coast in order to study the South-to-North gradient of the dust optical properties and the mixing processes with anthropogenic aerosols from the Balkan countries. The main goal of this study is the investigation of the more intense SD event occurred over Greece in recent years (Gerasopoulos et al., 2006) and the analysis of the spatial distribution of the dust optical properties along its way to and over Greece. This is accomplished by analyzing AOD_{550}, fine-mode fraction (FMF), aerosol index (AI), PM_{10} and AERONET data over different locations in Greece and investigating the agreement between columnar and surface measurements focusing mainly on dust event. In Section 2 the instrumentation and the data set are described, while in Section 3 the meteorological and atmospheric conditions are given for April 2005. The intense dust event of 16–17 April 2005 is examined in Section 4 analyzing both satellite and ground-based measurements.

2. Instrumentation and methods

2.1. MODIS sensor

MODIS has been acquiring daily global data in 36 spectral bands from visible to thermal infrared (29 spectral bands with 1-km resolution, five spectral bands with 500-m resolution, and two with 250-m resolution, nadir pixel dimensions). The MODIS sensor is onboard the polar orbiting NASA-EOS Terra and Aqua spacecrafts with equator crossing times of 10:30 and 13:30 Local Solar Time, respectively (Levy et al., 2007). The data used in this study include both Terra and Aqua-MODIS-derived AOD_{550} and FMF aerosol products, calculated using separate algorithms over land and ocean. Derived directly from the MODIS-observed spectral reflectance, the so-called Level 2 retrieval is calculated at a $10\,km \times 10\,km$ resolution (at nadir), representative of a 20×20 box of 500-m resolution data. Whether the box is over ocean or over land, specific logic is applied to screen clouds, ice/snow, and select which pixels should be considered to represent the $10\,km \times 10\,km$ area (Remer et al., 2005). Because of the sophisticated selection process, the MODIS retrieval can be performed near clouds, and may be valid even when the $10\,km \times 10\,km$ is 90% cloudy. At conclusion of the retrieval (either ocean or land), the products are assigned a 'quality assurance' (QA) value that indicates expected confidence or stability. As the Level 2 data are irregular in both space and time, a process for aggregation and averaging is required to make MODIS data efficient for comparing with other datasets. The resulting Level 3 MODIS products are available on daily and monthly intervals, globally, on a $1^\circ \times 1^\circ$ grid. It should be noted that depending on the MODIS-derived product, different weighting logic may be used to derive the Level 3 data products. In our case, we used the 'QA-weighted' daily Level 3 products, that are available from the Giovanni website (http://giovanni.gsfc.nasa.gov/).

While total AOD over ocean or land are defined the same way, FMF is different whether over ocean or over land. Over the ocean, the algorithm combines a single coarse mode (out of five choices) and single fine mode (out of four choices) to best match the MODIS-observed spectral reflectance. Over land, however, the algorithm matches a 'fine-dominated' aerosol (composed of fine and coarse modes), and a 'coarse-dominated' aerosol (also two modes) to

match the observed reflectance. Essentially, the FMF is the 'fine-dominated model fraction' indicating the relative importance of different aerosol regimes. Over the Eastern Mediterranean, in most seasons, the fine-dominated aerosol is assumed to have properties of a moderately absorbing aerosol (SSA ~ 0.9), while the coarse-dominated model is assumed to represent transported dust. As discussed in validation studies (e.g. Chu et al., 2002; 2003; Levy et al., 2003; Remer et al., 2002) a different expected uncertainty is applied to over ocean ($\pm 0.03 \pm 0.05$ AOD) and over land ($\pm 0.05 \pm 0.2$ AOD) retrievals. The application of sediment masks over ocean and NDVI masks over land reduces the errors traditionally associated with coastal regions (e.g. Remer et al., 2005). From tests on Mediterranean sites, Remer et al. (2002) indicated that particle-size properties may be retrievable over the ocean (e.g. effective radius to within 25%), but the FMF products cannot be considered 'validated' in the same way as AOD. In our study, we used both ocean and land Level 3 products from Collection 5 (Levy et al., 2007). The MODIS aerosol standard products (AOD_{550} and FMF) are provided in a spatial resolution of $1^\circ \times 1^\circ$ above the Eastern Mediterranean basin and correspond to Collection 5 (C005) Level 3 QA-weighted products data (Levy et al., 2007).

2.2. Aerosol Index

The Aerosol Index (AI) observed from the TOMS instrument is continued by the Ozone Monitoring Instrument (OMI) flown on the Finnish–Dutch EOS Aura spacecraft launched in July 2004 (Veihelmann et al., 2007). AI values from both sensors (TOMS on board Earth Probe and OMI on board Aura) were obtained in April 2005 over Eastern Mediterranean. However, there are mixed results with TOMS when dust and cloud are intermingled, even in theory, and it is very difficult to validate. The AI detects absorbing aerosols over all terrestrial surfaces including deserts and snow-ice covered surfaces. These aerosol types are also detected intermingled with clouds and above cloud decks. TOMS and OMI measure backscattered radiances in the UV region of the spectrum; from these measurements, the version 8 algorithm computes an absorbing AI, which is a qualitative measure of the presence of UV absorbing aerosols, such as mineral dust and smoke against non-absorbing aerosols, such as sea salt and sulfate particles (Torres et al., 1998). The AI indicates the presence of elevated absorbing aerosols in the troposphere. Because of this, the sensitivity of AI to aerosols increases more or less proportionally with the aerosol layer height, while any aerosol below about 1000 m is unlikely to be detected (Hsu et al., 1999). The absorbing AI is defined as the difference between the measured (including aerosol effects) spectral contrast at the 360- and 331-nm wavelength radiances; the contrast is calculated from the radiative transfer theory for a pure molecular (Rayleigh) atmosphere (Badarinath et al., 2007). From TOMS sensor the AI is available on a daily basis, on a 1° (latitude) by 1.25° (longitude) resolution. The TOMS Level 3 global gridded data set (new version 8 algorithm) on the $1.0^\circ \times 1.25^\circ$ grids used here are produced by the NASA TOMS Science Team (http://toms.gsfc.nasa.gov/). The new Aura-OMI level 2G daily gridded data products are generated by the NASA OMI science team by binning the original pixels from the Level 2 data products (15 orbits per day; 13-km × 24-km spatial resolution at nadir) into $0.25^\circ \times 0.25^\circ$ global grids. Therefore, the OMI-AI values have a greater spatial resolution than the TOMS-AI ones.

2.3. AERONET measurements

The AERONET measurements reported in this work were made with the CIMEL sunphotometer (CE-318), which is an automatic sun-sky scanning spectral radiometer. This instrument is installed at the FORTH-CRETE AERONET station, which is located at the Northern coast of Crete (35°19′N, 25°16′E), approximately 15 km East from Heraklion the largest city in Crete (Fotiadi et al., 2006). The CIMEL sunphotometer takes measurements of the direct sun and diffuse sky radiances every 15 min within the spectral range 340–1020 nm and 440–1020 nm, respectively. The direct-sun measurements are performed in eight spectral channels: 340, 380, 440, 500, 675, 870, 940 and 1020 nm. Seven of the eight bands are used to acquire AOD, while that at 940 nm is used to estimate the total precipitable water content. The Ångström parameter is computed from AODs at 440 and 870 nm. The filters utilized in these instruments are ion-assisted deposition interference filters with an FWHM of 10 nm except for the 340-nm and 380-nm filters having an FWHM of 2 and 4 nm, respectively. The instrumentation, data acquisition, retrieval algorithms and calibration procedure conform with the standards of the AERONET and are described in detail in numerous studies (e.g., Holben et al., 2001; Dubovik et al., 2000). Typically, the total uncertainty in AOD for a field instrument under cloud-free conditions, is ± 0.01 for $\lambda > 440$ nm, and ± 0.02 for shorter wavelengths. In this study, the daily-averaged Level 2 products, which are cloud-screened and quality assured (Smirnov et al., 2000), were used for April 2005.

2.4. PM_{10} measurements

The PM_{10} measurements over Greater Athens Area (GAA) are performed by the Ministry of Environment (MINENV) network. MINENV operates an organized monitoring network covering GAA with 18 stations, eight of which monitor aerosol concentrations, in terms of PM_{10}, on hourly basis. The examined data refer to hourly concentration measurements in April 2005, from which the daily-averaged values were obtained. PM_{10} filter samples are collected using low-volume samplers (US EPA-approved Partisol Model 2000). The sampling flow rate is 16.71 l min^{-1}. The particles are collected on 47-mm Pallflex TX40 l m^{-1} filters (Teflon-coated glass fiber filters), which are mounted in plastic filter holders. Each filter is inspected for its integrity prior to use. Particle concentrations are determined gravimetrically using an electronic microbalance (Metter Toledo AT201) with 0.01-mg resolution.

3. Summary of the aerosol fields over Greece in April 2005

Before focusing on the intense dust event of 16–17 April 2005, the AOD_{550} and FMF monthly variation obtained

from both Terra- and Aqua-MODIS sensors is analyzed. In Fig. 1 the daily values of AOD_{550} are given for April 2005 averaged over the area 32.0°–41.0° N and 20.0°–27.0° E, including continental Greece, Aegean Sea and Libyan Sea. The AOD_{550} varies widely from 0.175 to 1.94 for Terra-MODIS. The respective Aqua-MODIS values range from 0.21 to 2.42. The AOD_{550} values higher than 0.5 over the study area are mainly related to some SD events as revealed from HYSPLIT and DREAM models (not shown here) but are depicted with arrows in the figure. The dramatical increase in AOD_{550} values on 16–17 April clearly reveals the intensity of this dust event. Despite the difference in orbiting time and the fact that the data pixels from the two satellites are not always the same (due to differences in cloud cover), the Terra- and Aqua-MODIS sensors give similar AOD_{550} values, while a strong linear relation holds.

The three SD events occurring on 11–12, 16–17 and 25–26 April over the study region are clearly identified from the low FMF values from both sensors (Fig. 2). In April 2005 the FMF took values from relatively low (0.25–0.28), during the dust event on 17 April, to high (0.9–0.92) on 4 April, for Terra- and Aqua-MODIS, respectively. Above the whole Greek territory the FMF values show simultaneous presence of fine- and coarse-mode particles, with the fine mode to be dominant (mean values of 0.68 and 0.67 for Terra and Aqua, respectively). The large variability in FMF values is attributed to the variety of aerosol types and characteristics. It was found (not presented) that a strong North-to-South gradient in FMF values occurs. In contrast to AOD_{550}, the FMF values obtained from the two sensors are not correlated with great accuracy ($R^2 = 0.63$). However, no systematic overestimation or underestimation of any sensor is apparent. Nevertheless, in general, both sensors exhibit a similar day-to-day variation with concurrent maxima and minima.

In April, the aerosols are characterized by large differences in both their physicochemical and optical properties. Sea-spray and sulfate particles are the most common non-absorbing aerosols, while smoke particles with significant amount of black or organic carbon can have both absorbing

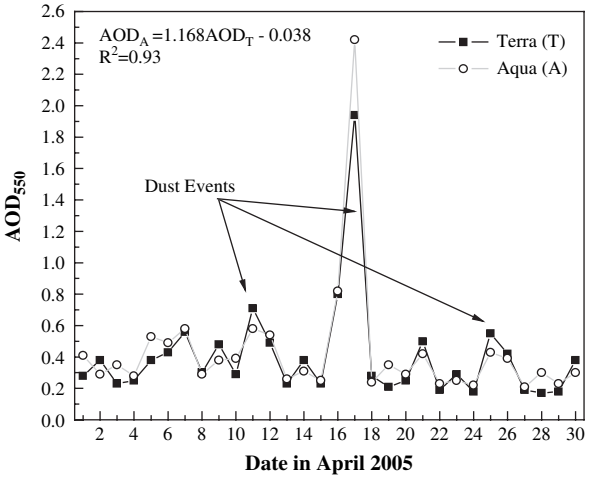

Fig. 1. AOD_{550} values obtained from Terra- and Aqua-MODIS sensors in April 2005 averaged over the area 32.0°–41.0° N, 20.0°–27.0° E.

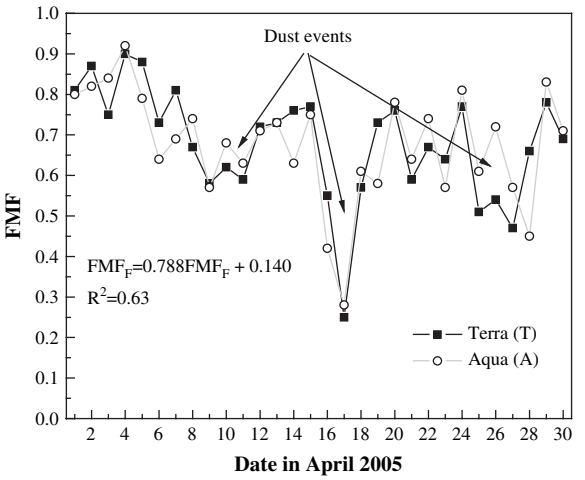

Fig. 2. Same as in Fig. 1, but for the FMF values.

and non-absorbing characteristics (Torres et al., 1998). Finally, mineral or dust aerosols represent the clearest possible absorbing signature (Israelevich et al., 2002). The detected high AOD_{550} from the satellites (Fig. 1) can be produced by the presence of either absorbing or non-absorbing particles and, therefore, additional information is necessary in order to assess both the detailed nature and the optical characteristics of this complex aerosol load over the region. For this reason the AI values derived by TOMS and averaged over the same area are given in Fig. 3 (lower panel) for April 2005. The daily values of the AI range from 0.01 to 1.58. These values correspond to the mixture of absorbing aerosols (dust or soot particles), which are expected to affect the whole area. The highest values are observed during dust events, which are shown with arrows. Significant positive correlations between AI with PM_{10} and AOD_{550} from both Terra and Aqua are observed for April 2005 over Athens, which are analyzed in detail in Section 5. On the other hand, the AI presents negative correlations with FMF values for the same period above the Greek territory, while the linear relations are statistically significant at the 95% confidence level. Thus, the linear regressions of the forms $AI = -1.89FMF + 1.73$ ($R^2 = 0.48$), and $AI = -1.76FMF + 1.64$ ($R^2 = 0.41$) for Terra and Aqua, respectively, hold. These negative correlations are expected, since the AI takes higher values in the dust events when the FMF values are minimum. On the other hand, on days with local pollution from anthropogenic fine-mode aerosols (large FMF values), the AI values are relatively low since the AI cannot detect urban aerosols within the boundary layer (Torres et al., 1998).

The analysis of the measured UV radiation via remote sensors has become a pivotal point in extracting information about aerosols in recent years (Koukouli et al., 2006). Thus, the local noon UV erythemal (UV_{ery}) irradiance derived by TOMS above the same area is also given in Fig. 3. As expected, an increasing trend in UV_{ery} occurs mainly due to a change in solar zenith angle. The UV_{ery} is also strongly affected by the columnar ozone amount and, for this reason, the ozone variation is also given in the

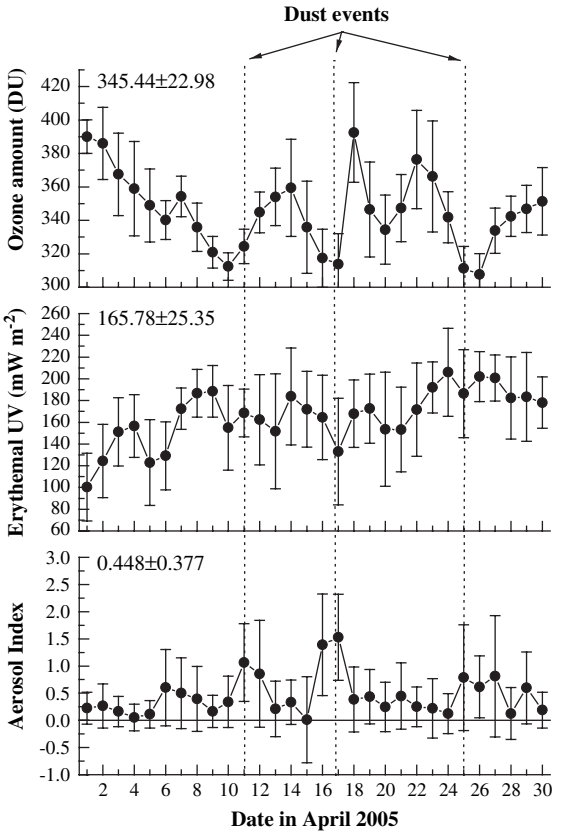

Fig. 3. Same as in Fig. 1, but for the total-ozone columnar amount, UV_{ery} and AI values derived by TOMS on board the Earth Probe satellite.

figure. However, the relation between UV_{ery} and ozone column is out of scope of the present study and also presents high scatter ($R^2 = 0.12$). Nevertheless, we can focus on the dust events, when the ozone amount exhibits its lowest values. Under normal conditions, one would expect that the quite low ozone value on 17 April (intense dust event) would cause an increase in the $UV_{ery.}$ In contrast, the UV_{ery} on that day exhibits low values directly influenced by the intense Sahara dust load. This fact highlights the strong attenuation of the UV irradiance by dust. This feature was also underlined by di Sarra et al. (2002) and Balis et al. (2004) and is mainly attributed to the highest absorbing efficiency of dust particles in the UV due to their chemical composition. Because of the large decrease in UV, and in general in global radiation reaching the ground, the dust plumes exhibit a great potential in the radiative transfer in the atmosphere. Nevertheless, the correlations between UV_{ery} with AOD_{550}, AI and FMF in April 2005 are very low ($R^2 < 0.10$), since the UV_{ery} also depends on ozone amount and solar zenith angle.

The scatterplot of AOD_{550} against FMF is shown in Fig. 4 for April (lower panel) and for 17 April (upper panel). Such relations between AOD and FMF allow inferences to be made on the aerosol types (Kaskaoutis et al., 2007a). The data correspond to mean monthly values (April 2005) at each pixel covering the area 32°–41° N, 20°–27° E. For whole April, 73 pixel values are correlated, which are fewer

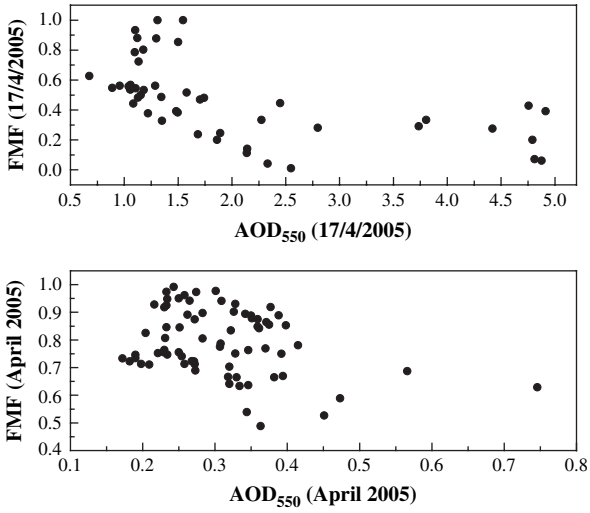

Fig. 4. Correlation between AOD_{550} and FMF values derived by Aqua-MODIS over the area 32°–41° N, 20°–27° E. Upper panel for 17/4/2005, lower panel for April 2005 (mean values).

(49) on 17 April due to cloud presence (see Figs. 5 and 7). On monthly basis there is a wide range of FMF values (~0.5 to 1.0) for $AOD_{550} < 0.4$, associated with low-to-moderate turbidity conditions, involving various types of particles, such as natural sulfate maritime aerosols, mineral or desert dust, soot, anthropogenic particles or photochemical pollution. The scatterplot on 17 April is characteristic for the presence of coarse-mode aerosols, since for high AOD_{550} values (>1.6) the FMF values are quite low (below 0.4).

4. Focus on the SD event of 16–17 April 2005

4.1. Spatial distribution of the dust plume

In this section the analysis is focused on the dust event on 16–17 April 2005, which was one of the most intense above Greece in the last decades (Gerasopoulos et al., 2006). Remotely-sensed aerosols via satellite images give general picture and can provide information of the spatial distribution of the aerosol properties. In Fig. 5 the Aqua-MODIS true-color image on 17 April 2005 (11:40 UTC) is given. The thick dust plume (as a yellow veil) is well depicted, being transported from Libya over the Eastern Mediterranean and specifically Greece, covering an extended area. The dust layer also traveled over the Balkan countries (not shown in the figure). This yellow veil is evident in between the North African coast and Crete; then it becomes more vague as being diluted by the removal processes (mainly dry deposition). The residence time of the SD particles varies significantly; their distribution is highly variable in space and time. This is the reason why remote sensing of aerosols has made great progress, as is the best technique to catch individual events (of Saharan outbreaks in this case) and to integrate them into regional or global images of aerosol transport. Nevertheless, polar-orbiting satellite monitoring is limited in

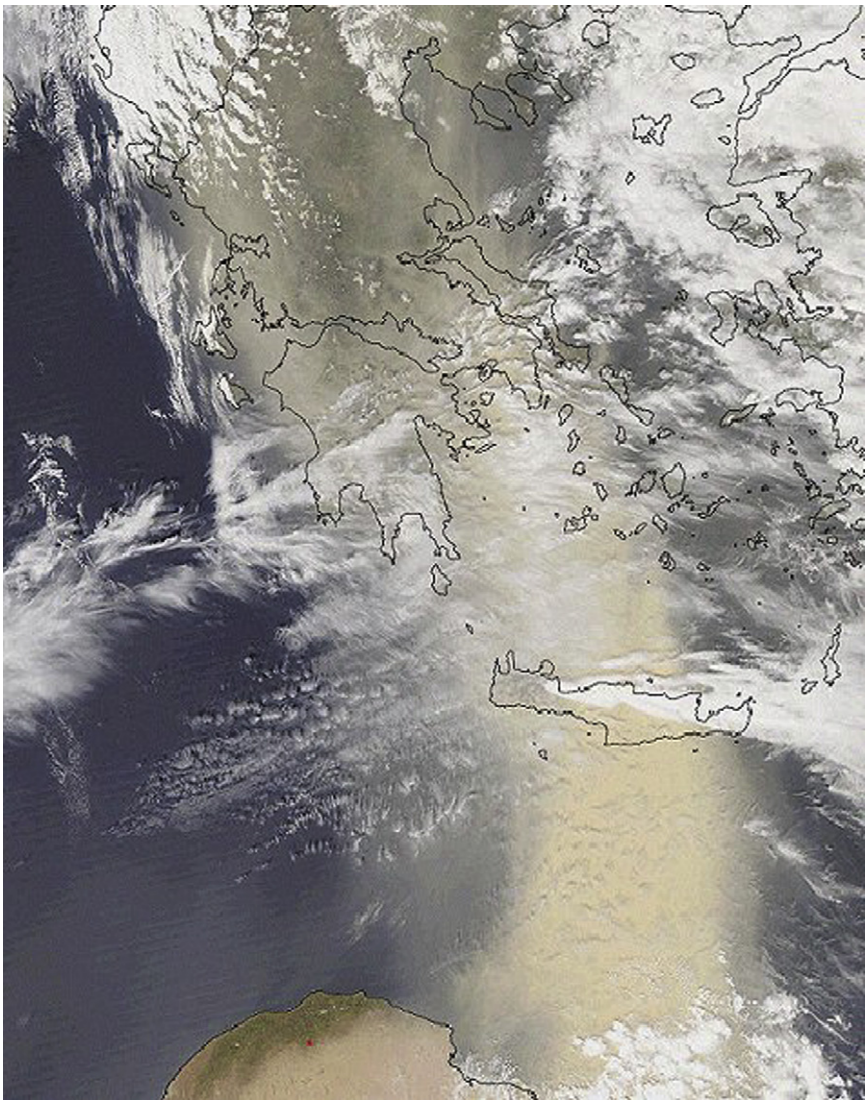

Fig. 5. True-color image obtained from Aqua-MODIS sensor on 17 April 2005 (11:40 UTC).

describing the evolution of aerosol transport and only provides instantaneous images with sparse time resolution. Significant cloud cover is also obvious on 17 April; as a consequence, the elevated dust plume may interact with cloud microphysical properties (cloud condensation nuclei, cloud albedo, water-vapor content) altering them. It is well known that dust interacts with clouds, after absorbing hygroscopic material (Levin et al., 1996), and affects photolysis rates and ozone chemistry by modifying the spectrum of UV radiation (Zerefos et al., 2002). Dust over Greece comes mostly from Southwest as several studies show (Papayannis et al., 2005; Fotiadi et al., 2006). In contrast, the present SD event comes directly from South as being transported from Libya. This fact, in conjunction with the dust intensity and its long-distance transport, makes its analysis very interesting.

The Aqua-MODIS AOD_{550} and FMF values as well as the OMI and TOMS-AI ones obtained via Giovanni website are shown in Fig. 6a, b, c, and d, respectively. This figure covers the whole Eastern Mediterranean in order to reveal the spatial distribution of the aerosol properties during the SD event. The white gaps in MODIS figures correspond to lack of data due to cloud contamination. In Fig. 6a, the high AOD_{550} values clearly indicate the dust plume, which covers Eastern Mediterranean and Greece and extends to the Balkan counties. Especially over Athens the AOD_{550} values on 17 April are around 2.0, causing reduction in visibility, degradation of the air quality and adverse effects on human health. In Central Mediterranean the aerosol load is rather low, practically unaffected by the dust storm. The low FMF values (Fig. 6b) indicate the presence of coarse-mode particles along the dust pathway. These low FMF values are also present in Central Balkans further indicating the intensity and the long-range transport of the dust event. In relation with the MODIS data, the OMI-AI values (Fig. 6c) show the presence of highly absorbing aerosols in the UV over the

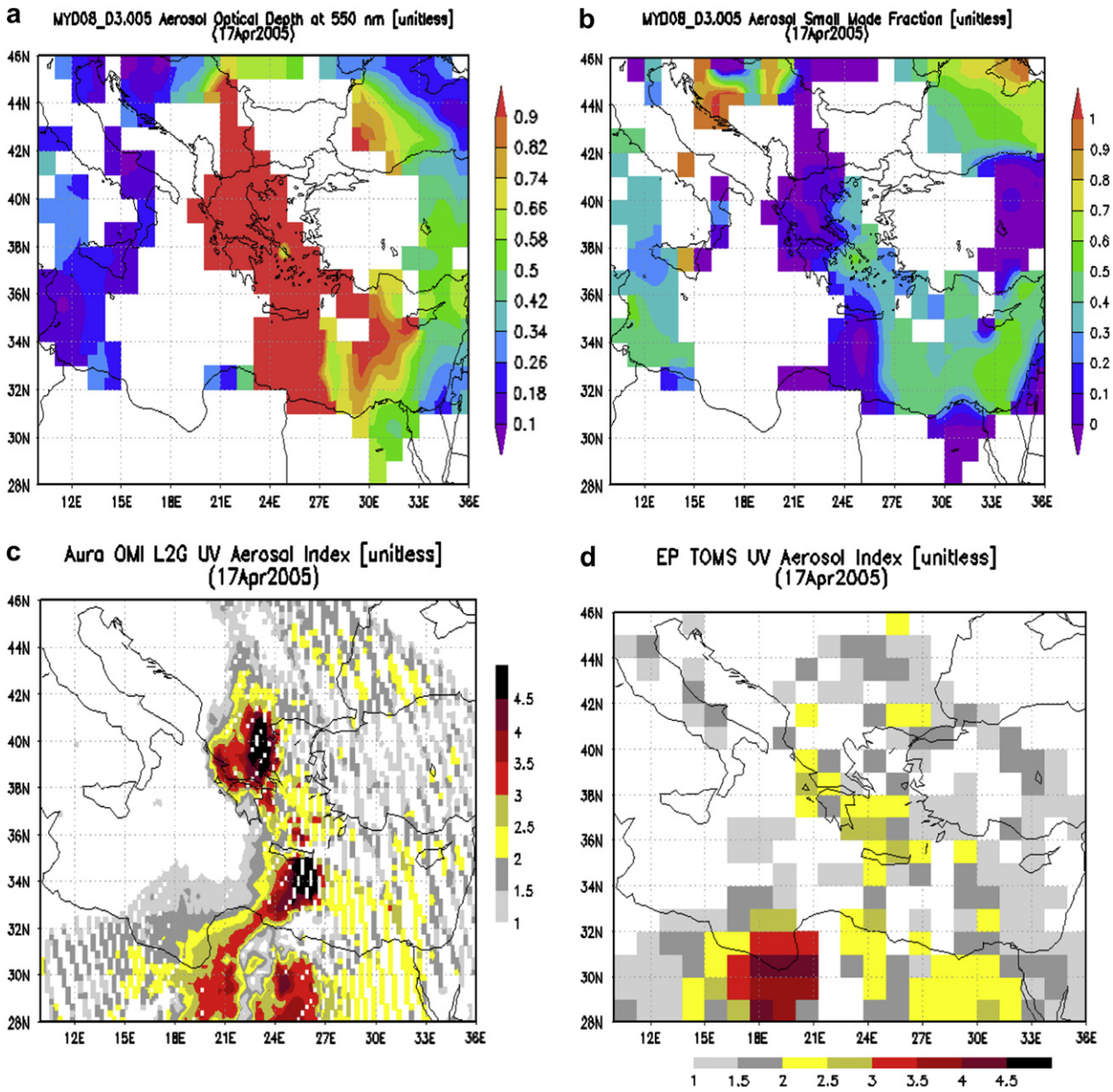

Fig. 6. Aqua-MODIS values on 17 April 2005 above Eastern Mediterranean, (a) AOD_{550}, (b) FMF, (c) OMI-AI and (d) TOMS-AI.

region. Such high AI values correspond to thick dust layers (Torres et al., 1998; Koukouli et al., 2006). The respective TOMS image (Fig. 6d) shows significantly lower AI values over Eastern Mediterranean and Greece. On 17 April 2005 no forest fires were detected from MODIS and, therefore, the high AI values over Eastern Mediterranean and Greece are attributed to the dust presence.

4.2. Regional meteorology

In general, the wind fields are found to be particularly useful in evaluating the transport of Sahara dust over Eastern Mediterranean and Greece. The synoptic meteorological conditions on 17 April 2005 appear in Fig. 7. More specifically, in the lower troposphere, the spatial distribution of Geopotential Height at 850 hPa (Fig. 7a) shows the presence of a low located in Central Europe. As a consequence, the established circulation brings air masses from Libya (which is at the South periphery of the low) to Greece with gale winds (16–19 m s^{-1}) as depicted in Fig. 7b. Sahara desert dust is transported to the North, covering a wider area from Libya to Northern Greece. This situation is amplified in the middle troposphere, where an extended trough at 500 hPa Geopotential Height (Fig. 7c) centered in Northern Italy, resulted in Southwestern circulation over Greece. The wind field at 500 hPa Geopotential Height appeared in Fig. 7d, reveals that violent stormy winds (29–30 m s^{-1}) blow from Southwestern direction, strengthening

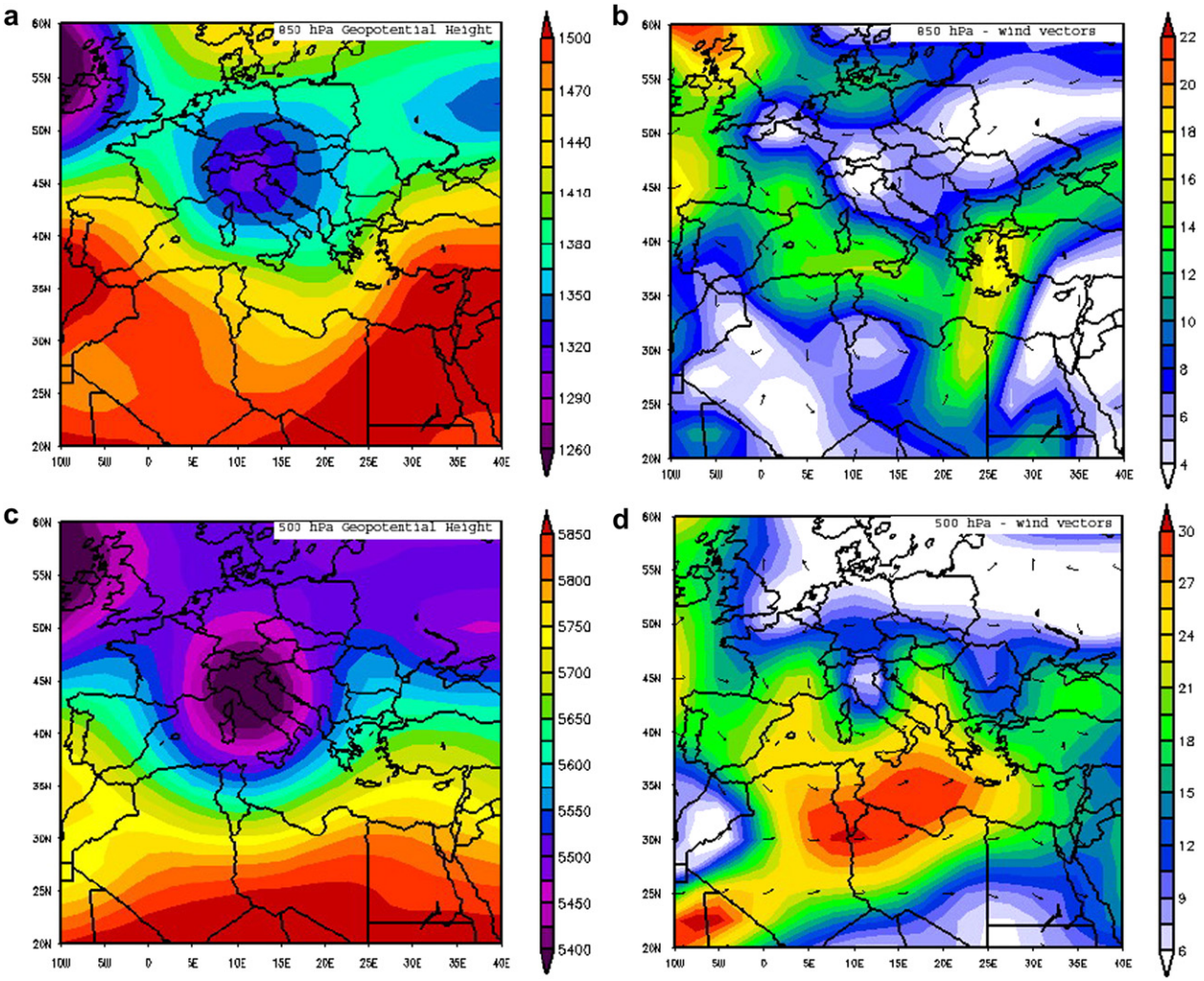

Fig. 7. Spatial distribution of the 850 hPa Geopotential Height in m, (a), wind vectors ($m\,s^{-1}$) at 850 hPa (b), 500 hPa Geopotential Height in m (c) and wind vectors ($m\,s^{-1}$) at 500 hPa (d), on 17 April 2005, from NCEP/NCAR reanalysis.

the SD transportation at the middle troposphere, towards Greece. In addition, the back-trajectory pattern (not shown) suggests a prevalent Southern flow in the whole atmospheric column (500, 1500 and 4000 m), since transport of dust occurs vertically. This atmospheric structure is more common in spring, carrying heavily dust-loaded air masses over Greece (Kalivitis et al., 2007). The warm region in Sahara indicates the occurrence of surface heating and uplift of warm air, which is associated with a strong convection and consequent uplift of dust particles driven by the surface heating. The uplift of air masses from the Sahara desert through convection towards Southern Europe and Greece can be verified from the 4000-m trajectory (not shown). Furthermore, this is a typical synoptic configuration allowing for the transport of Saharan dust to Central Mediterranean and Southern Italy (Barkan et al., 2005; Meloni et al., 2008). Barkan et al. (2005) identified a low-pressure system over the Iberian Peninsula and West African coast and a subtropical high-pressure system as the two main features that influence the transport of dust from Africa to Europe. Moreover, Escudero et al. (2007) identified a similar pattern as the most frequent and effective in case of dust outbreaks over the Western Mediterranean and Iberia. Meloni et al. (2008) found that the above-described meteorological situation produced the most favorable conditions for intense SD outbreaks at Lampedusa.

4.3. Optical properties of the dust plume transport

In this Section the dust plume optical properties are further investigated along the dust pathway from the Libyan coast to the Balkan countries. The MODIS data (AOD_{550} and FMF) are analyzed (as longitudinal averages over the dust-plume area 22–25° E) with respect to the latitude. Therefore, Fig. 8 allows one to observe the changes in the dust-plume characteristics and the coating with other aerosol types along its pathway. Even though the

uncertainties in satellite sensors can be high under specific areas and circumstances (e.g., highly reflecting surfaces, land-ocean sub-pixel contamination, presence of clouds, non-spherical dust particles) the retrieval algorithm of the Collection 5 (C005) has been significantly validated and developed nowadays (Levy et al., 2007). Thus, the values given in Fig. 8 can be assumed quite accurate.

A clear South-to-North gradient is obvious regarding the AOD_{550} values (lower panel), thus underlining the attenuation of dust load along its path towards Greece and Balkan countries. After its exposure from Libya coast the intense dust plume is continuously attenuated since heavier particles gradually being scavenged inside the boundary layer, while only the smaller ones can reach Northern Greece and Bulgaria (42° N). The residence time of the dust aerosols depends on the meteorological conditions, mainly wind speed and precipitation that effect dry and wet aerosol deposition, respectively (Papayannis et al., 2005). Nevertheless, the remaining high AOD_{550} values (>1.0) at the Northern latitudes clearly indicate the intensity of this SD event.

The Eastern Mediterranean and Aegean Sea is a crossroad of aerosols from different sources and types (maritime aerosols, desert dust particles, urban pollution and seasonal biomass burning). As a consequence, the dust optical and physical characteristics can easily be misquoted after coating with other aerosol types (e.g., sulfate) over coastal and continental Europe (Levin et al., 1996). To the contrary, the dust optical properties after intense Asian outflows can be detected over large distances above the Pacific Ocean reaching the western USA (Fairlie et al., 2007). Also, the dry deposition of the most heavy desert particles and their contamination by other aerosol types (like biomass burning at the coasts of Algeria in the summer months) may play a crucial role in modifying the dust aerosol properties and their vertical distribution (Meloni et al., 2007). The presence of urban/industrial anthropogenic aerosols, either from local sources or transported via polluted air masses from Europe, are identified by the higher FMF values at the Northern latitudes. Kaskaoutis et al. (2007b) showed that such cases occur mainly in spring and are associated with Northern-sector winds, carrying polluted air masses from Central, Eastern Europe and Balkan countries or local stagnant air masses enriched with industrial emissions. More particularly, for latitudes higher than Thessaloniki the identification of a dust plume according to the criteria set by Kaskaoutis et al. (2007b) is problematic. The presence of dust over Greece is mainly related to long-range transport extended vertically up to 4 km (Papayannis et al., 2005) and thus it can be identified by satellites. Israelevich et al. (2002) examined the occurrence of desert dusts in the Mediterranean using TOMS data. To this respect, the AI values obtained by TOMS and OMI sensors are analyzed for 17 April 2005 (Fig. 9). Both values are averaged over the longitudes 22°–25.5° E. The main conclusion of this figure is that the sensors give significantly different AI values over the area, as well as high spatial inhomogeneity. The OMI gives higher mean AI values (2.30 ± 0.78) compared to the mean of 1.43 ± 0.59 given by TOMS. Kalivitis et al. (2007) presented high TOMS-AI values (>2.0) under Saharan dust events over Crete. Furthermore, the AI values from both sensors do not seem to decrease along the dust pathway, since high AI values can be depicted over Northern latitudes, especially from OMI. In contrast, TOMS gives slightly lower values for latitudes above 40°. However, high AI values can also be detected by the presence of highly absorbing urban aerosols (Koukouli et al., 2006) and a significant fraction (~35%) of dust outbreaks over Eastern Mediterranean has no signal on AI values (Kalivitis et al., 2007).

The significant spatial inhomogeneity of the dust plume can further be seen in Fig. 10a–c, where the Engström exponent in the 550–865 nm band, the aerosol effective radius (R_{eff}) and the mass concentration are presented, respectively. These

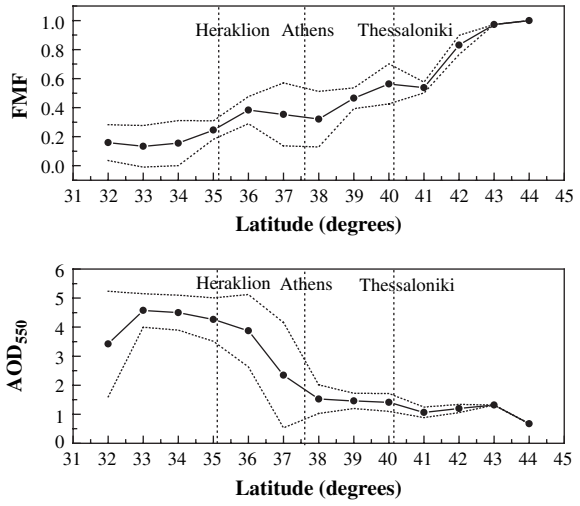

Fig. 8. The attenuation of dust plume on 17/4/2005 along its pathway. The AOD_{550} (lower panel) and FMF (upper panel) data were derived from Aqua-MODIS and averaged over the longitudes 22°–25° E. The dotted lines represent the standard deviation of the mean. The latitudes of Heraklion (Crete), Athens and Thessaloniki are also shown in the figures.

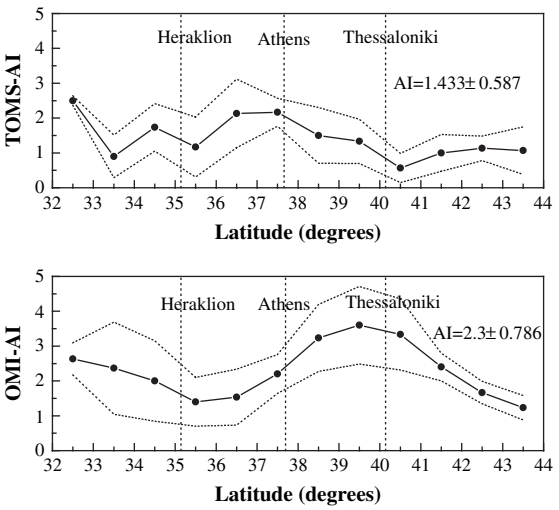

Fig. 9. Same as in Fig. 8, but for AI values derived from OMI (lower panel) and TOMS (upper panel).

figures refer to aerosol optical properties above ocean using the ocean MODIS algorithm, which is more accurate than the land algorithm (Levy et al., 2007). All the aforementioned remarks regarding the spatial inhomogeity, the strong South-to-North gradient in dust aerosol characteristics, the deposition of large and heavy particles along the dust-plume trajectory and possible mixing with other aerosol types are verified in Fig. 10. Thus, the Engström exponent (Fig. 10a) shows very low (near to zero), or even negative $\alpha_{550-865}$ values South of Crete, where the dust layer is very thick (see Fig. 1). This fact verifies the presence of large dust particles, since their R_{eff} is above 2.0 in this area (Fig. 10b). North of Crete, where the heaviest dust particles were deposited, thus the thinner dust layer in Fig. 1, the Angstrom exponent is higher. It is worth noticing the larger values close to Athens probably caused by the local anthropogenic emissions. In accordance with the Engström exponent, the R_{eff} continues to decrease towards Northern Greece. In addition, due to the removal mechanisms, the aerosol composition and concentration are highly variable, since the spatial distribution of the aerosol mass concentration (Fig. 10c) is very pronounced, with very high values South of Crete and significant lower in the Northern latitudes. It should be noticed The great agreement in the spatial distribution between the mass concentration retrievals (Fig. 10c) and the satellite image (Fig. 1) should be noticed. The high difference in the above parameters for areas North or South of Crete can be attributed to the dry deposition of aerosols since the PM_{10} measurements reached $\sim 2500\,\mu g\,m^{-3}$ on 17 April in Crete, compared to those of $\sim 250\,\mu g\,m^{-3}$ in Athens.

The daily mean AOD data at selected wavelengths (380, 500, 675 and 870 nm) derived from the FORTH-CRETE AERONET station in April 2005 are given in Fig. 11. In

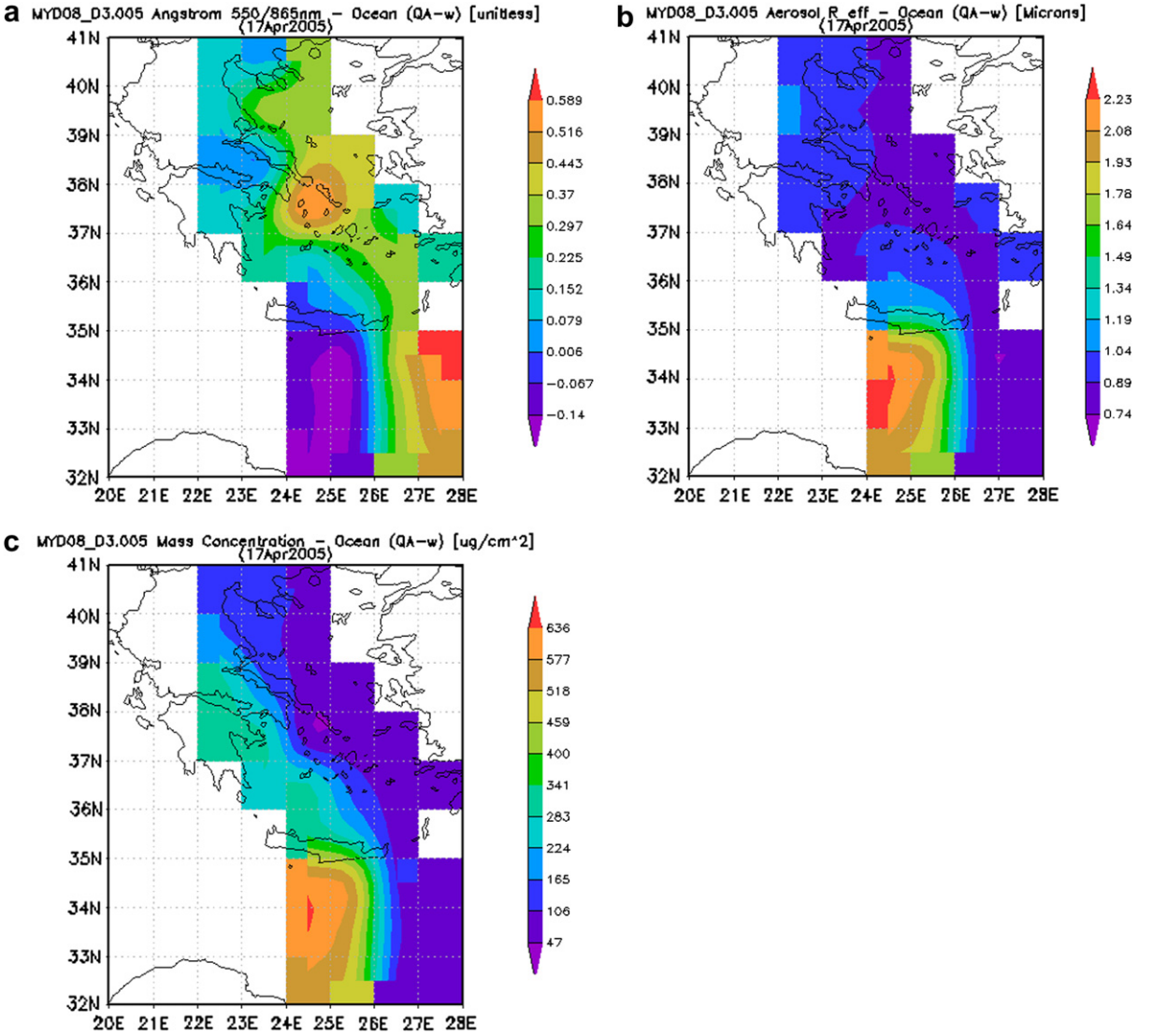

Fig. 10. Spatial distribution of (a) Angstrom exponent in the 550–865 nm band, (b) aerosol effective radius and (c) aerosol mass concentration on 17 April 2005. The figures were derived from Aqua-MODIS sensor and refer to retrievals over ocean according to the MODIS ocean algorithm.

the same figure the α-Ångström values in the range 440–870 nm are also shown for the same period. In general, the AOD temporal pattern is in close agreement with the respective from MODIS (Fig. 1). On the first days of April the high AOD values are associated with local or transported pollution (high $\alpha_{440-870}$ values). On 11 April the AODs start to increase with concurrent decrease of the α values (first dust event). Very high AOD increase is depicted on 16 April, when the intense dust event influences the area. The third dust event on 25–26 April is also apparent from the AERONET data of the FORTH-CRETE station. Unfortunately, the cloud presence over the station on 17 April did not permit AERONET measurements. It would be very interesting to have information of the AODs on that day, in order to compare them with the corresponding satellite values. The high AOD values as well as the dust events in this period are reported by Gerasopoulos et al. (2006), who also analyzed the dust-particle chemical composition.

In Fig. 12 the daily mean PM_{10} concentrations averaged for the eight monitoring stations in GAA are presented for April 2005. The main anthropogenic sources of PM_{10} within GAA are vehicular traffic, central heating, industrial and construction activities. Along with Saharan dust, a natural contribution to the total PM_{10} concentration is expected from Aeolian and traffic-driven resuspension, biogenic and marine aerosols, as reported by Gobbi et al. (2007) for Rome. The significant variability in PM_{10} concentrations within GAA is attributed to the local characteristics of each sampling station (e.g., urban, suburban, traffic, etc.). The current Greek and European Union (EU) legislations employ PM_{10} records as one of the reference parameters to assess urban air quality (Gobbi et al., 2007). Furthermore, health effects due to elevated concentrations of the total suspended particles are harmful and have been estimated in several studies (Rodriguez et al., 2001; Prospero et al., 2002). According to the EU standards, from 1 January 2005, the exceedance of the daily-average threshold of

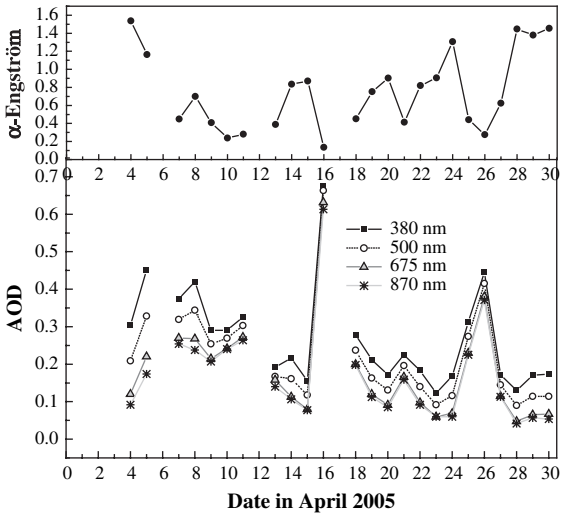

Fig. 11. Spectral AOD and Engström exponent values in the range 440–870 nm from the FORTH-CRETE AERONET station in April 2005.

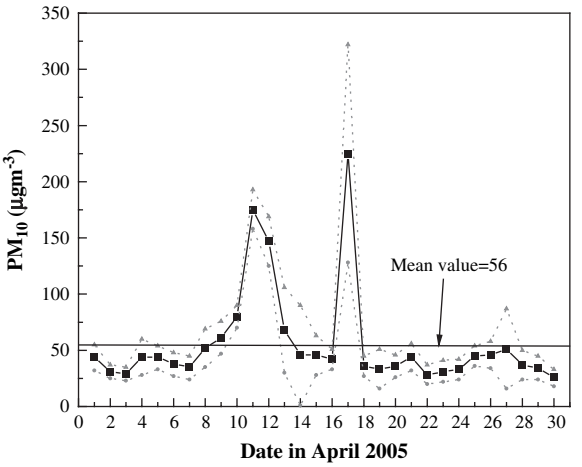

Fig. 12. Mean and standard deviations of the daily-averaged PM_{10} concentrations from eight air pollution monitoring stations located in the Greater Athens Area. The mean April value is also given.

50 μg m^{-3} at any station is allowed for a maximum of 35 times per year, while the PM_{10} annual average should not exceed 40 μg m^{-3}. These are rather ambitious goals considering the current levels of PM_{10} observed in Athens, not to mention the dramatic increase of the PM_{10} levels in the presence of dust.

The average 24-h PM_{10} concentrations regarding all stations within GAA during April 2005 is 56.2 ± 41.3 μg m^{-3}, which is considerably higher than the EU 2001 air quality annual PM_{10} standard of 40 μg m^{-3}. A previous study by Chaloulakou et al. (2003) showed that the monthly mean PM_{10} concentrations in GAA ranged from 63.6 μg m^{-3} (January) to 88.9 μg m^{-3} (December) with an annual mean value of 75.5 μg m^{-3}. Daily mean PM_{10} concentrations exceeded the daily EU limit of 50 μg m^{-3} for 9 days in April 2005. It was found that on 6 of those the air masses came from Africa carrying significant amounts of dust. On 11–12 April the SD advection over Athens led to a PM_{10} increase of ~100 μg m^{-3} compared to the April mean value, while on 17 April this increase was about 150 μg m^{-3}, thus exceeding the 50 μg m^{-3} EU limit. This fact shows that the dust transported over Greece in the vertical atmospheric column has a direct impact on the boundary layer aerosol load. Unfortunately, there are no lidar observations on 17 April due to thick dust layer near the ground, which obscured the measurements. However, lidar signals in Athens on 18 April show significant amount of aerosols in the whole atmospheric column and especially near the ground, confirming the high PM_{10} concentrations.

In Heraklion, Crete, the PM_{10} concentrations were very high reaching 250 μg m^{-3} (hourly values) as a result of South–Southeast winds on 11–12 April (Gerasopoulos et al., 2006). On 16–17 April, the intense dust event directly influenced the PM_{10} concentrations on the ground. As reported by Gerasopoulos et al. (2006) the maximum PM_{10} values at Finokalia, Crete, reached 2500 μg m^{-3}, while at Heraklion the upper limit of the measuring instrument (1000 μg m^{-3}) was approached. Despite the fact that

long-range advection takes place mainly above the boundary layer, subsidence, fumigation and sedimentation cause a large deal of the dust to diffuse into it (Gobbi et al., 2007). Therefore, mineral dust, not only originating from Sahara, is expected to play an important role on the total mass of suspended particulate matter measured at surface in coastal Mediterranean areas (Chaloulakou et al., 2003; Gerasopoulos et al., 2006).

5. Conclusions

This study analyzed an intense SD event occurred over Eastern Mediterranean and Greece on 16–17 April 2005 using satellite observations and ground-based measurements. In April 2005 three dust events were identified above the area, strongly influencing the aerosol load and the PM_{10} concentrations on the surface. Both Terra- and Aqua-MODIS sensors indicated the dust outflows. In addition, during the dusty days the AI values derived from TOMS and OMI sensors exhibited higher values. Especially on 17 April the AOD_{550} values reached or even surpassed the value of 2.0 above Eastern Mediterranean. In close agreement, the FMF on that day exhibited its lowest values (0.25–0.28). The SD event on 17 April was clearly evident via satellite true-color images as an intense dust plume originating from Libya, traversing the Mediterranean and arriving over Greece and the Balkan countries. The dust characteristics along its pathway from the African coast to continental Europe showed significant spatial inhomogeneity, since the larger particles were deposited near the source and the smaller transported to long distances. As a consequence, the AOD_{550} continuously decreased along the dust pathway. On the other hand, the mixing of the dust particles with anthropogenic aerosols over continental Europe had a clear effect on the increase of the FMF values. The AERONET data from Crete clearly indicated the dust transport on certain days in April 2005. Athens had quite high average PM_{10} levels and, therefore, the presence of mineral dust contributed to exceeding the EU thresholds. As a consequence, on the dusty days of April 2005, the daily mean PM_{10} concentrations in Athens reached 150 $\mu g\,m^{-3}$ on 11–12 April and over 200 $\mu g\,m^{-3}$ on 17 April. The ground-based measurements were found to be in close agreement with the satellite ones. This fact indicates how efficiently the satellite sensors can monitor specific events. The combined use of satellite with sunphotometer measurements, regional dust models, particle samplers and lidar systems, sounds very appropriate for the dust transport investigation.

Acknowledgments

The authors would like to thank the MODIS science data support team (past and present) for processing data via the Giovanni website (http://giovanni.gsfc.nasa.gov/) and more particularly Dr. Robert Levy for information about the algorithm and retrieval processes of the collection C005 MODIS data set and helpful criticism of the article. Also, the HYSPLIT and NCEP reanalysis scientific teams are acknowledged for providing the meteorological fields. In addition, we would like to thank Dr. M. Drakakis for his effort in establishing and maintaining the AERONET FORTH-CRETE site. Finally, the Greek Ministry of Environment, Physical Planning and Public Works for disposing the PM_{10} concentration measurements used in this work, and the lidar team of the National Technical University of Athens for providing the lidar profiles on 18 April 2005.

References

d' Almeida, G.A., 1986. A model for Saharan dust transport. J. Climatol. Appl. Meteorol 25, 903–916.

Alpert, P., Kishcha, P., Shtivelman, A., Krichak, S.O., Joseph, J.H., 2004. Vertical distribution of Saharan dust based on 2.5-year model predictions. Atmos. Res. 70, 109–130.

Antoine, D., Nobileau, D., 2006. Recent increase of Saharan dust transport over the Mediterrenean Sea, as revealed from ocean color satellite (SeaWiFS) observations. J. Geophys. Res. 111, D12214. doi:10.1029/2005JD006795.

Balis, D.S., Amiridis, V., Zerefos, C.S., Kazantzidis, A., Kazadzis, S., Bais, A.F., Meleti, C., Papayannis, A., Matthias, V., Dier, H., Andreae, M.O., 2004. Study of the effect of different type of aerosols on UV-B radiation from measurements during EARLINET. Atmos. Chem. Phys. 4, 307–321.

Badarinath, K.V.S., Kumar Kharol, Shailesh, Kaskaoutis, D.G., Kambezidis, H.D., 2007. Dust storm over Indian region and its impact on the ground reaching solar radiation – a case study using multi-satellite data and ground measurements. Sci. Total Environ. 384, 316–332.

Barkan, J., Alpert, P., Kutiel, H., Kishcha, P., 2005. Synoptics of dust transportation days from Africa toward Italy and central Europe. J. Geophys. Res. 110, D07208. doi:10.1029/JD006795.

Chaloulakou, A., Kassomenos, P., Spyrelis, N., Demokritou, P., Koutrakis, P., 2003. Measurements of PM_{10} and $PM_{2.5}$ particle concentrations in Athens, Greece. Atmos. Environ. 37, 649–660.

Chu, D.A., Kaufman, Y.J., Ichoku, C., Remer, L.A., Tanre, D., Holben, B.N., 2002. Validation of MODIS aerosol optical depth retrieval overland. Geophys. Res. Lett. 29. doi:10.1029/2001GL013205.

Chu, D.A., Kaufman, Y.J., Zibordi, G., Chem, J.D., Mao, J., Li, C., Holben, B.N., 2003. Global monitoring of air pollution over land from the earth observing system-terra moderate resolution imaging spectroradiometer (MODIS). J. Geophys. Res. 108 (D21), 4661. doi:10.1029/2002JD003179.

Claquin, T., Schulz, M., Balkanski, Y., Boucher, O., 1998. Uncertainties in assessing radiative forcing by mineral dust. Tellus B 50, 491–505.

Donaghay, P.L., Liss, P.S., Duce, R.A., Kester, D.R., Hanson, A.K., Villareal, T., Tindale, N.W., Gifford, D.J., 1991. The role of episodic atmospheric nutrient inputs in the chemical and biological ecosystems. Oceanography 4, 62–70.

Dubovik, O., Smirnov, A., Holben, B.N., King, M.D., Kaufman, Y.J., Eck, T.F., Slutsker, I., 2000. Accuracy assessments of aerosol properties retrieved from Aerosol Robotic Network (AERONET) sun and sky radiance measurements. J. Geophys. Res. 105, 9791–9806.

Dunion, J., Velden, C., 2004. The impact of the Saharan air layer on Atlantic tropical cyclone activity. Bull. Am. Meteor. Soc. 85, 353–365.

Escudero, M., Querol, X., Avila, A., Cuevas, E., 2007. Origin of the exceedances of the European daily PM limit value in the regional background areas of Spain. Atmos. Environ. 41, 730–744.

Fairlie, T.D., Jacob, D.J., Park, R.J., 2007. The impact of transpacific transport of mineral dust in the United States. Atmos. Environ. 41, 1251–1266.

Fotiadi, A., Hatzianastassiou, N., Drakakis, E., Matsoukas, C., Pavlakis, K.G., Hatzidimitriou, D., Gerasopoulos, E., Mihalopoulos, N., Vardavas, I., 2006. Aerosol physical and optical properties in the Eastern Mediterranean Basin, Crete, from Aerosol Robotic Network data. Atmos. Chem. Phys. 6, 5399–5413.

Gerasopoulos, E., Kouvarakis, G., Babasakalis, P., Vrekoussis, M., Pataud, J.-P., Mihalopoulos, N., 2006. Origin and variability of particulate matter (PM_{10}) mass concentrations over the Eastern Mediterranean. Atmos. Environ. 40, 4679–4690.

Gobbi, G.P., Barnaba, F., Ammannato, L., 2007. Estimating the impact of Saharan dust on the year 2001 PM_{10} record of Rome, Italy. Atmos. Environ. 41, 261–275.

Holben, B.N., Tanre, D., Smirnov, A., Eck, T.F., Slutsker, I., et al., 2001. An emerging ground-based aerosol climatology: aerosol optical depth from AERONET. J. Geophys. Res. 106, 12,067–12,097.

Hsu, N.C., Herman, J.R., Torres, O., Holben, N.B., Tanre, D., Eck, T.F., Smirnov, A., Chatenet, B., Lavenu, F., 1999. Comparisons of the TOMS aerosol index with sunphotometer aerosol optical thickness: results and applications. J. Geophys. Res. 104, 6269–6279.

IPCC, 2007. Summary for policymakers. In: Solomon, S., Qin, D., Manning, M., Chen, Z., Marquis, M., Averyt, K.B., M.Tignor, Miller, H. L. (Eds.), Climate Change 2007: The Physical Science Basis. Contribution of Working Group I to the Fourth Assessment Report of the Intergovernmental Panel on Climate Change. Cambridge University Press, Cambridge, United Kingdom/New York, NY, USA.

Israelevich, P.L., Levin, Z., Joseph, J.H., Ganor, E., 2002. Desert aerosol transport in the Mediterranean region as inferred from the TOMS aerosol index. J. Geophys. Res. 107 (D21), 4572. doi:10.1029/2001JD002011.

Kalivitis, N., Gerasopoulos, E., Vrekousis, M., Kouvarakis, G., Kubilay, N., Hatzianastassiou, N., Vardavas, I., Mihalopoulos, N., 2007. Dust transport over the Eastern Mediterranean from TOMS, AERONET and surface measurements. J. Geophys. Res. 112, D03202. doi:10.1029/2006JD007510.

Kaskaoutis, D.G., Kambezidis, H.D., Hatzianastassiou, N., Kosmopoulos, P., Badarinath, K.V.S., 2007a. Aerosol climatology: on the discrimination of the aerosol types over four AERONET sites. Atmos. Chem. Phys. Discuss. 7, 6357–6411.

Kaskaoutis, D.G., Kosmopoulos, P., Kambezidis, H.D., Nastos, P.T., 2007b. Aerosol climatology and discrimination of different types over Athens, Greece based on MODIS data. Atmos. Environ. 41, 7315–7329.

Kaufman, Y.J., Tanrè, D., Boucher, O., 2002. A satellite view of aerosols in the climate system. Nature 419, 215–223.

Kinne, S., Pueschel, R., 2001. Aerosol radiative forcing for Asian continental outflow. Atmos. Environ. 35, 5019–5028.

Koukouli, M.E., Balis, D.S., Amiridis, V., Kazadsis, S., Bais, A., Nickovic, S., Torres, O., 2006. Aerosol variability over Thessaloniki using ground based remote sensing observations and the TOMS aerosol index. Atmos. Environ. 40, 5367–5378.

Levin, Z., Ganor, E., 1996. The effects of desert particles on cloud and rain formation in the Eastern Mediterranean. In: Guerzoni, S., Chester, R. (Eds.), The Impact of Desert Dust Across the Mediterranean. Springer, New York, pp. 77–86.

Levin, Z., Ganor, E., Gladstein, V., 1996. The effects of desert particles coated with sulphate on rain formation in the eastern Mediterranean. J. Appl. Meteorol. 35, 1511–1523.

Levy, R.C., Remer, L.A., Tanre, D., Kaufman, Y.J., Ichoku, C., Holben, B., Livingston, J., Russell, P., Mating, H., 2003. Evaluation of the MODIS retrievals of dust aerosol over the ocean during PRIDE. J. Geophys. Res. 108. doi:10.1029/2002JD002460.

Levy, R.C., Remer, L.A., Dobovik, O., 2007. Global aerosol optical properties and application to Moderate Resolution Imaging spectroradiometer aerosol retrieval over land. J. Geophys. Res. 112, D13210. doi:10.1029/2006JD007815.

Meloni, D., di Sarra, A., Biavati, G., DeLuisi, J.J., Monteleone, F., Pace, G., Piacentino, S., Sferlazzo, D.M., 2007. Seasonal behavior of Saharan dust events at the Mediterranean island of Lampedusa in the period 1999–2005. Atmos. Environ. 41, 3041–3056.

Meloni, D., di Sarra, A., Monteleone, F., Pace, G., Piacentino, S., Sferlazzo, D.M., 2008. Seasonal transport patterns of intense Saharan dust events at the Mediterranean island of Lampedusa. Atmos. Res. 88, 134–148.

Moulin, C., Lambert, C.E., Dayan, U., et al., 1998. Satellite climatology of African dust transport in Mediterranean atmosphere. J. Geophys. Res. 103, 13137–13144.

Ogunjobi, K.O., He, Z., Simmer, C., 2008. Spectral aerosol optical properties from AERONET Sun-photometric measurements over West Africa. Atmos. Res. 88, 89–107.

Papayannis, A., Balis, D., Amiridis, V., Chourdakis, G., Tsaknakis, G., Zerefos, C.S., Castanho, A.D.A., Nickovic, S., Kazadzis, S., Grabowski, J., 2005. Measurements of Saharan dust aerosols over the Eastern Mediterranean using elastic backscatter-Raman lidar, spectrophotometric and satellite observations in the frame of the EARLINET project. Atmos. Chem. Phys. 5, 2065–2079.

Prospero, J.M., Ginoux, P., Torres, O., Nicholson, S.E., Gill, T., 2002. Environmental characterization of global sources of atmospheric soil dust identified with Nimbus 7 Total Ozone Mapping Spectrometer (TOMS) absorbing aerosol product. Rev. Geophys. 40. doi:10.1029/2000RG000095.

Remer, L.A., Tanre, D., Kaufman, Y.J., Ichoku, C., Matoo, S., Levy, R., Chu, D.A., Holben, B., Dubovik, O., Ahmad, Z., Smirnov, A., Martins, J.V., Li, R.R., 2002. Validation of MODIS aerosol retrieval over ocean. Geophys. Res. Lett. 29. doi:10.1029/2001GL013204.

Remer, L.A., et al., 2005. The MODIS aerosol algorithm, products, and validation. J. Atmos. Sci. 62, 947–973.

Rodriguez, S., Querol, X., AlastueyKallos, G., Kakaliagou, O., 2001. Saharan dust contributions to PM_{10} and TSP levels in Southern and Eastern Spain. Atmos. Environ. 35, 2433–2447.

di Sarra, A., Cacciani, M., Chamard, P., Cornwall, C., DeLuisi, J.J., Di Iorio, T., Disterhoft, P., Fiocco, G., Fuà, D., Monteleone, F., 2002. Effects of desert dust and ozone on the ultraviolet irradiance at the Mediterranean island of Lampedusa during PAUR II. J. Geophys. Res. 107 (D18), 8135. doi:10.1029/2000JD000139.

Satheesh, S.K., Krishna Moorthy, K., 2005. Radiative effects of natural aerosols: a review. Atmos. Environ. 35, 2089–2110.

Smirnov, A., Holben, B.N., Eck, T.F., Dubovik, O., Slutsker, I., 2000. Cloud screening and quality control algorithms for the AERONET data base. Remote Sens. Environ. 73, 337–349.

Torres, O., Bhartia, P.K., Herman, J.R., Ahmad, Z., Gleason, J., 1998. Derivation of aerosol properties from satellite measurements of backscattered ultraviolet radiation: theoretical basis. J. Geophys. Res. 103, 17,099–17,110.

Veihelmann, B., Levelt, P.F., Stamnes, P., Veefkind, J.P., 2007. Simulation study of the aerosol information content in OMI spectral reflectance measurements. Atmos. Chem. Phys. 7, 3115–3127.

Zerefos, C.S., Kourtidis, K.A., Melas, D., et al., 2002. Photochemical activity and solar ultraviolet radiation (PAUR) modulation factors: an overview of the project. J. Geophys. Res. 107 (D18), 8134.